Identification of Nonpeptidic Urotensin II Receptor Antagonists by Virtual Screening Based on a Pharmacophore Model Derived from Structure−Activity Relationships and Nuclear Magnetic Resonance Studies on Urotensin II

Stefanie Flohr,[†] Michael Kurz,[†] Evi Kostenis,[‡] Alexandre Brkovich,[§] Alain Fournier,[§] and Thomas Klabunde*[,†]

Lead Generation Chemistry, Aventis Pharma Germany GmbH, Industriepark Hoechst, D-65926 Frankfurt am Main, Germany, Disease Group Cardiovascular, Aventis Pharma Germany GmbH, Industriepark Hoechst, D-65926 Frankfurt am Main, Germany, and Centre de Recherche en santé humaine, Institut Armand-Frappier, Université du Québec, Pointe-Claire, Quebec, Canada

Received November 15, 2001

The vasoactive cyclic 11-amino acid peptide urotensin II (U-II) has recently been discovered as the endogenous ligand of the orphan G-protein-coupled receptor GPR14. As U-II might be involved in the regulation of cardiovascular homeostasis and pathology, a nonpeptidic GPR14/U-II antagonist is of considerable basic and therapeutic interest. We have performed structure−activity relationship studies on U-II by investigating 25 peptide analogues to mobilize intracellular calcium in GPR14-transfected CHO cells, demonstrating that only the side chains of the residues Trp-7, Lys-8, and Tyr-9 are required for receptor recognition and activation. The solution structure of U-II derived by nuclear magnetic resonance has served as a structural template for a three-dimensional three point pharmacophore query for the virtual screening of the Aventis compound repository for nonpeptidic U-II receptor antagonists. Highly active lead compounds of six different scaffold classes could be identified, antagonizing the biological activity of U-II in vitro. The most potent compound identified by the virtual screening approach, 1-(3-carbamimidoyl-benzyl)-4-methyl-1H-indole-2-carboxylic acid (naphthalen-1-ylmethyl)amide, reveals an IC_{50} of 400 nM in a functional fluorometric imaging plate reader assay and constitutes a promising lead.

Introduction

Urotensin II (U-II) is an 11-amino acid cyclic peptide found in diverse species, including humans.[1] The C-terminal cyclic heptapeptide part (CFWKYCV) from U-II, which is essential for the biological activity,[2] has been highly conserved in evolution from fish to mammals.[3]

The cloning of cDNA encoding human U-II[1] and the identification of this peptide as the endogenous ligand for the orphan receptor GPR14[4−7] have stimulated interest in the potential physiological and pathophysiological role of human U-II. Ames et al. reported that GPR14 is mainly expressed in the cardiovascular system. Strikingly, systemic administration of U-II to anaesthesized monkeys caused intense vasoconstriction followed by fatal cardiovascular collapse. These spectacular observations led the authors to conclude that U-II may be involved in the regulation of cardiovascular homeostasis and pathology. In vitro, U-II isopeptides are characterized by their potent and sustained vasoconstrictor activity in a wide variety of mammalian blood vessels among others from rats,[8] dogs,[9] and, most importantly, humans.[10,11]

Although the biology of U-II and GPR14 is still in its infancy, the precedence set by more established vasoactive polypeptides, e.g., angiotensin-II or endothelin-1, suggests that the U-II system offers a great potential for the identification and development of novel therapeutic strategies related to the treatment of cardiovascular diseases. To elucidate the definitive (patho)-physiological role of UII/GPR14 in the control of cardiovascular function, the development of suitable tool compounds, e.g., nonpeptide U-II receptor antagonists, will be of significant utility. We report herein the exploitation of classical structure−activity relationship (SAR) studies and nuclear magnetic resonance (NMR) spectroscopy to identify pharmacophoric elements within U-II that serve as a starting point for the identification of small molecule U-II receptor ligands in a virtual screening approach.

Results and Discussion

SAR of hU-II. Analogues of hU-II were designed, synthesized by Echaz microcollections (Tübingen, Germany) using standard solid phase techniques, and evaluated for their ability to mobilize intracellular calcium in CHO cells transiently transfected with human U-II receptor.

The first series of U-II peptides (Table 1) was designed to elucidate the role of the exocyclic aa for receptor interaction. Toward this goal, a stepwise truncation of the exocyclic aa was performed. As can be taken from Table 1, analogues 2−5 were equally potent and efficacious as native hU-II. These data are in agreement with the report of Itoh[2] who showed that the highly conserved C-terminal part of U-II (CFWKYCV) is the minimal sequence required to retain full activity at the Gillich-

* To whom correspondence should be addressed. Tel.: +49 69 305 14355. Fax: +49 69 33 1399. E-mail: Thomas.Klabunde@aventis.com.
[†] Lead Generation Chemistry, Aventis Pharma Germany GmbH.
[‡] Disease Group Cardiovascular, Aventis Pharma Germany GmbH.
[§] Université du Québec.

10.1021/jm0111043 CCC: $22.00
Published on Web 03/20/2002

Table 1[a]

no.	peptide	sequence	EC_{50} (nM)	E_{max}
1	U-II (1−11)	ETPDCFWKYCV	2.5 ± 0.2	100
2	U-II (2−11)	TPDCFWKYCV	2.4 ± 0.1	103 ± 3.8
3	U-II (3−11)	PDCFWKYCV	3.6 ± 0.6	100 ± 5.5
4	U-II (4−11)	DCFWKYCV	3.0 ± 0.9	102 ± 4.5
5	U-II (5−11)	CFWKYCV	1.8 ± 0.3	106 ± 4.0
6	U-II (1−10)	ETPDCFWKYC	1.8 ± 0.1	99 ± 3.5
7	U-II (5−10)	CFWKYC	2.3 ± 1.1	95 ± 6.8

[a] Mobilization of intracellular calcium by U-II and truncated U-II peptides in CHO cells transiently transfected with the human U-II receptor. Changes in intracellular calcium were recorded in intact cells, loaded with Fluo4 as described in detail in the Experimental Section. Potencies of the peptides are given as EC_{50} values in nanomolar ± SEM from two to five independent concentration−response curves. Maximum responses (E_{max} values) produced by peptides are expressed as percent of the maximum response induced by native hU-II.

Table 2[a]

no.	sequence	EC_{50} (nM)	E_{max}
8	**A**TPDCFWKYCV	1.8 ± 0.3	101 ± 1.7
9	E**A**PDCFWKYCV	3.3 ± 0.8	101 ± 0.7
10	ET**A**DCFWKYCV	1.9 ± 0.8	102 ± 3
11	ETP**A**CFWKYCV	2.7 ± 0.5	101 ± 3
12	ETPD**A**FWKYCV (linear)	233 ± 16	96 ± 4
13	ETPDC**A**WKYCV	5.7 ± 0.3	98 ± 1
14	ETPDCF**A**KYCV	1,303 ± 98	45 ± 2
15	ETPDCFW**A**YCV	14,800 ± 800	ND
16	ETPDCFWK**A**CV	193 ± 9	75 ± 3
17	ETPDCFWKYC**A**	3.2 ± 0.3	99 ± 2

[a] Functional characterization of U-II peptides, in which individual aa were replaced by Ala residues. Additional experimental details are described in Table 1.

thys U-II receptor. In contrast to the results of Itoh for U-II from Gillichthys, not only truncation of exocyclic aa at the N terminus but also truncation of the C-terminal Val is without effect on activity at the human U-II receptor as exemplified by peptide 6 (hU-II (1−10)) and peptide 7 (hU-II (5−10)). Peptide 7 representing only the disulfide-bridged cyclic hexapeptide of hU-II is equipotent as compared with native hU-II. Thus—although the C-terminal Val has been highly conserved during evolution—it is dispensable for activation of the human U-II receptor but not of the Gillichthys U-II receptor. In pharmacological studies using rat aortic strips, U-II (5−10) shows about 1000-fold lower activity as compared to full-length U-II.[12,13]

To further delineate the structural requirements of U-II for receptor activation, we systematically replaced each residue in hU-II by alanine. The sequence of these peptides and their biological activities in the functional in vitro assay are shown in Table 2.

In accordance with our results from the truncation scan, replacement of any exocyclic residue of U-II by Ala does not affect the potency and efficacy of the peptides (peptides 8−11 and 17). However, if aa of the conserved hexacyclic part are replaced by Ala, dramatic increases in EC_{50} values are observed: peptide 14 displays 520-, peptide 15 displays 6000-, and peptide 16 displays 80-fold lower activity as compared with U-II. In addition to a decrease in agonistic potency, these analogues reveal an impaired efficacy of ligand−receptor interaction. They are partial agonists, which do not fully activate the U-II receptor.

In contrast, substitution of Phe by Ala in peptide 13 results only in a 2-fold increase in EC_{50}, with peptide 13 still a full receptor agonist. These results suggest that the sequence WKY in the cyclic part is most important for full agonistic activity of hU-II, whereas the evolutionarily highly conserved Phe only plays a minor role.

Table 3[a]

no.	sequence	EC_{50} (nM)	E_{max}
18	ETPDC-WKYCV	53 + 2	67 ± 1
19	ETPDCF-KYCV	>10 000	ND
20	ETPDCFW-YCV	not active	ND
21	ETPDCFWK-CV	not active	ND

[a] Functional characterization of U-II peptides, in which individual aa of the cyclic structure were deleted. Additional experimental details are described in Table 1.

Table 4[a]

no.	sequence	EC_{50} (nM)	E_{max}
22	ETPDC**f**WKYCV	1003 ± 98	87 ± 1
23	ETPDCF**w**KYCV	3.8 ± 0.5	98 ± 3
24	ETPDCFW**k**YCV	>10 000	ND
25	ETPDCFWK**y**CV	not active	ND

[a] Functional characterization of U-II peptides, in which individual L-aa within the cyclic structure have been replaced by their D counterparts. Additional experimental details are described in Table 1.

This hypothesis is further sustained by analogues with deletions inside the cyclic structure (Table 3). All analogues with truncation of only one aa in the cyclic part yielding a cyclic pentapeptide lose their activity with the exception of ETPDCWKYCV (peptide18), where the message sequence WKY is present. Although peptide 18 has considerable agonistic potency, it is not able to fully activate the receptor. In contrast, deletion of any other aa of the message sequence results in a complete loss of activity as shown in Table 3.

Replacement of Cys-6 by Ala (peptide 12, Table 2) yields a linear peptide with low activity. Obviously, the disulfide bridge stabilizes a conformation, which is essential for full biological activity. In this respect, U-II resembles other cyclic peptides such as somatostatin,[14] vasopressin,[15] and melanin-concentrating hormone (MCH)[16,17] in which the cyclic structure is crucial for their agonistic activity on the respective receptor.

To explore the importance of the correct conformation of the message sequence, we switched the chirality of the amino acids in the cyclic part (Table 4). In fact, substitution of aa in the hexacyclic part by the corresponding D-aa (peptides 22, 24, and 25) causes a dramatic decrease of the observed agonistic activities. Surprisingly, replacement of L-Trp by D-Trp (peptide 23) is tolerated without a significant change of the EC_{50} value.

In summary, our SAR studies allow us to derive the message sequence WKY representing the part of the physiological ligand essential for the biological activity. This finding is in agreement with the SAR studies performed by Kinney et al. on goby UII.[18]

The amino acid side chains of the message sequence of U-II represent chemical key features, which, in the correct spatial arrangement, are the prerequisite for binding of U-II and activation of the U-II receptor. To translate the information of the message sequence into a three-dimensional (3D) pharmacophore query suitable for virtual screening, we determined the conformation of hU-II in aqueous solution by NMR spectroscopy.

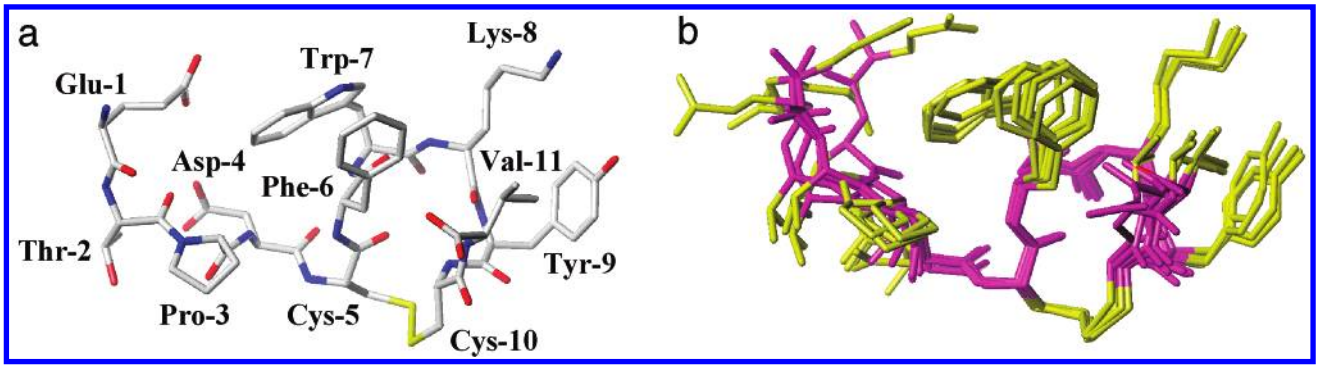

Figure 1. (a) Structure of U-II obtained after 350 ps of restrained MD simulation and energy minimization. Protons are not shown for clarity. (b) Superposition of six structures of U-II. During a 300 ps MD simulation, structures were sampled every 50 ps and energy-minimized. All backbone heavy atoms of Pro-3 to Cys-10 were used as reference points. Protons are not shown for clarity.

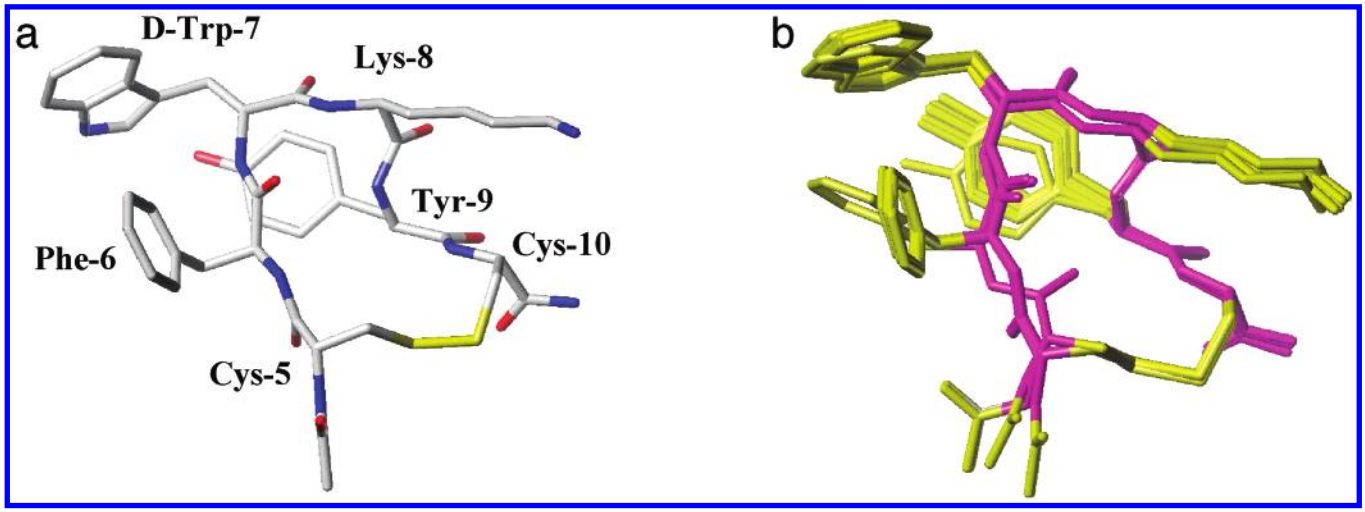

Figure 2. (a) Structure of Ac-CFwKYC-NH_2 obtained after 550 ps of restrained MD simulation and energy minimization. Protons are not shown for clarity. (b) Superposition of 10 structures of Ac-CFwKYC-NH_2. During a 500 ps MD simulation, structures were sampled every 50 ps and energy-minimized. All backbone heavy atoms were used as reference points. Protons are not shown for clarity.

It is well-known that amino acids with D-configuration support the formation of β-turn type structures resulting in conformationally restricted peptides. The experimentally accessible solution structure of a conformationally restricted peptide represents a good model for its bioactive receptor-bound conformation. Therefore, the 3D solution structure of a conformationally restricted peptide, which retains the biological activity, can serve as a structural template for a 3D pharmacophore model for virtual screening. From our SAR studies, it was known that the exchange of Trp by D-Trp at position 7 of U-II is tolerated without significant loss of activity. Therefore, we designed and synthesized the disulfide-bridged hexapeptide Ac-CFwKYC-NH_2 as a second tool compound for NMR studies. Although this compound is 200-fold less active than native hU-II (data not shown), it is still a potent human U-II receptor agonist.

NMR Structures of hU-II and Analogues. The ^{1}H resonance assignment of U-II and Ac-CFwKYC-NH_2 was performed following the standard procedure described by Wüthrich.[19] The analyses of the ROESY spectra revealed 57 distance constraints for U-II and 32 for the hexapeptide, respectively, which were used as input for the restrained molecular dynamics (MD) calculations. The results of these calculations are shown in Figures 1 and 2.

For U-II, the average root mean square (rms) deviation over all heavy atoms is 1.50 Å with a maximum deviation of 1.91 Å (Figure 1). Including only backbone heavy atoms, the average rms deviation is 1.04 Å with a maximum deviation of 1.39 Å. However, most of this relatively large deviation is due to flexibility in the linear parts of the peptide, whereas the cyclic part including the side chains of the message sequence is much better defined (i.e., the average rms deviation of the backbone heavy atoms including only residues Pro-3 to Cys-10 is 0.45 Å with a maximum deviation of 0.57 Å). No classical turn structure or intramolecular hydrogen bond is observed for the cyclic part of U-II. This is in accordance with a previous NMR study on telostean fish U-II in dimethyl sulfoxide (DMSO).[20]

The NMR data of Ac-CFwKYC-NH_2 reveals that the structure of the hexapeptide is very well-defined (including the side chains of the message sequence), which is reflected by an average rms deviation of 0.66 Å over all heavy atoms with a maximum deviation of 0.96 Å (Figure 2). Including only backbone heavy atoms, the average rms deviation is 0.27 Å with a maximum deviation of 0.71 Å. In contrast to U-II, the structure is characterized by a distorted β-II′ turn with D-Trp in position $i + 1$. Furthermore, the side chain orientation of especially Tyr-9 differs significantly from the one obtained in U-II. The NMR structures of both peptides

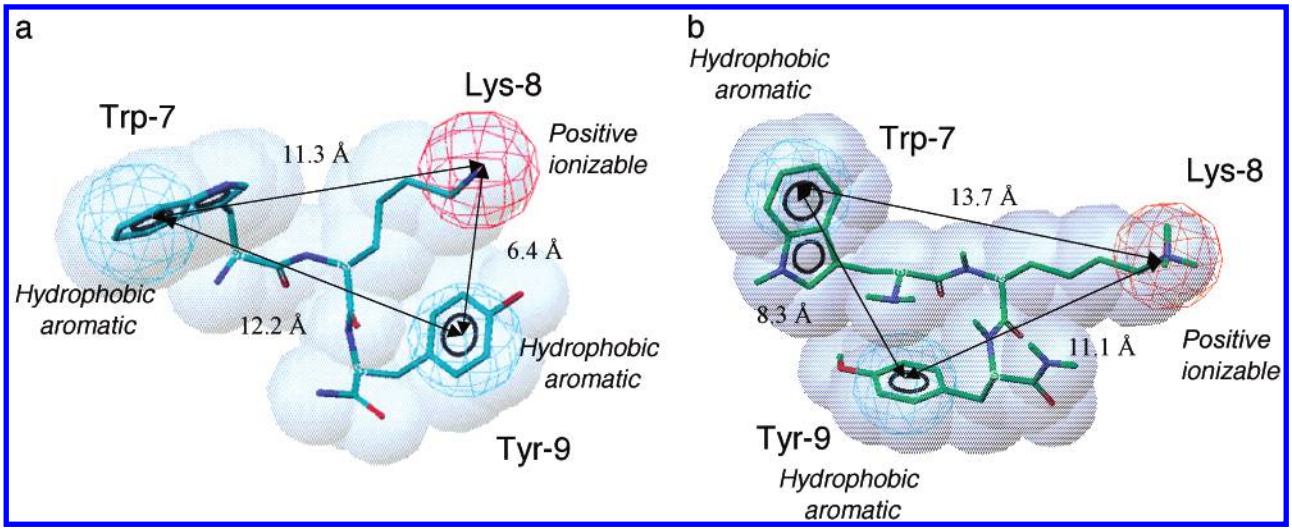

Figure 3. Pharmacophore query used for virtual screening of Aventis compound collection mapped onto bioactive fragment of NMR structure of (a) U-II and (b) Ac-CFwKYC-NH_2. The light blue spheres represent the two hydrophobic aromatic features; the red sphere represents the positive ionizable feature of the three point 3D pharmacophore (location restraint 1.5 Å). The gray spheres display the shape requirements linked to the pharmacophore query. Distances between the pharmacophoric points are shown in Ångstroms.

have been used as a template for the generation of a 3D-pharmacophore query for the virtual screening approach.

Virtual Screening. The SAR studies presented within this paper have revealed that the sequence WKY within U-II is essential for binding and activation of the receptor. Exchange of any of these three message sequence residues by alanine leads to a dramatic loss of potency and efficacy of the corresponding peptide in the functional in vitro U-II assay. These results indicate that the hydrophobic side chains of Trp-7 and Tyr-9 as well as the positive charge of Lys-8 represent key elements for U-II activation. Under the assumption that the NMR-derived solution structure of U-II can serve as a model for the receptor-bound conformation of U-II, we used the conformation of U-II in solution as a template to generate a three point pharmacophore hypothesis (Figure 3a): A positive ionizable feature has been placed on the Nϵ atom of Lys-8, and two hydrophobic aromatic features have been positioned onto the aryl rings of Trp-7 and Tyr-9, respectively. The distances between the pharmacophoric points are given in Figure 3a.

To further improve our pharmacophore hypothesis, we searched for U-II derivatives, which retain the high efficacy of the physiological ligand but are conformationally restricted. For these conformationally restricted peptides, it can be assumed that the receptor-bound conformation is similar to their solution structure. Truncation of U-II to the cyclic core and exchange of Trp against D-Trp yields the hexapeptide Ac-CFwKYC-NH_2, which reveals a good efficacy in the functional in vitro assay (though 200-fold reduced as compared to U-II). This peptide has been proposed on the basis of molecular modeling data as a putative UII receptor antagonist[13] but was shown by Nothacker et al. to behave like an agonist with a 190-fold lower potency as compared with natural U-II.[7] As expected, the NMR study of this hexapeptide in solution reveals that the introduction of the D-amino acids stabilizes a type β-II′ turn conformation with the D-amino acid in position $i + 1$. The NMR solution structure of this moderately active peptide has been used as a template to generate a second three point pharmacophore hypothesis (Figure 3b): The positive ionizable feature has been placed on the Nϵ atom of Lys-8, and two hydrophobic aromatic features have been positioned onto the aryl rings of Trp-7 and Tyr-9, respectively. The distances between the pharmacophoric points are given in Figure 3b.

Further attempts to rigidify the message sequence have been made by synthesis of backbone-cyclized hexapeptides (e.g., cycloAFwKY, cycloAFwKYA, and cycloAFwKYa). However, these peptides reveal only moderate activity (EC_{50} 3.7, 4.3, and 23.8 μM, respectively) and have therefore not proven to be useful as templates to generate further three point pharmacophore queries.

Using the two three point pharmacophore hypothesis, the Aventis compound repository has been virtually screened to select those compounds that fulfill the pharmacophoric and spatial requirements of the queries. The virtual screening of the Aventis compound database has yielded 500 compounds matching the U-II-based pharmacophore and 418 compounds matching the hexapeptide-based pharmacophore. The biological activity of these 918 virtual hits against the U-II receptor was tested in a functional fluorometric imaging plate reader (FLIPR) assay. Only one of 418 compounds identified using the hexapeptide-based pharmacophore showed an IC_{50} below 10 μM. The hit rate of 0.2% (number of active compounds/number of compounds tested $\times$ 100) is only barely higher than hit rates seen in high throughput screens for GPCR antagonists. This result indicates that the NMR-derived conformation of the hexapeptide is not an appropriate model for the receptor-bound conformation of the physiological ligand.

Biological testing of 500 compounds matching the U-II-based pharmacophore revealed 10 compounds (hit rate of 2%), which inhibit the U-II-induced calcium signal with IC_{50} values ranging from 400 nM to 7 μM. The verified virtual hits belong to six different scaffold classes. The largest class comprises four compounds and

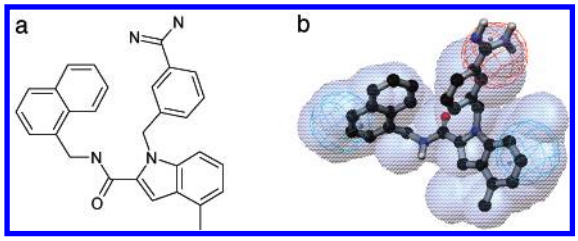

Figure 4. (a) Representative compound S6716 with EC_{50} of 400 nM in the functional FLIPR assay resulting from the virtual screen of the Aventis compound library. (b) Mapping of S6716 onto pharmacophore based on NMR structure of U-II. A similar orientation as in Figure 3a has been chosen.

is represented by amidated indolic acids, which have a benzamidine subsitutent at the indolic nitrogen. The good mapping of the most active compound of this class S6716 (IC_{50} 400 nM, Figure 4a) carrying a naphthalenmethylamine group as a substituent at the indolic acid is shown in Figure 4b: The phenyl ring of the indole of S6716 and the naphthyl ring of the naphthalenmethylamine side chain are mapping onto the two aromatic hydrophobic features of the pharmacophore. The amidino group of the benzamidine ring in S6716 superimposes with the positive ionizable feature of the 3D query.

Nine of 11 verified virtual hits fulfill the "rule of five"[21] and are therefore promising starting points for a drug discovery program. Our most active class, the substituted indoles, shows generally high metabolic stability in human S9 cell lines (>90%), but its predicted human absorption determined by Caco-2 cell lines is low (1%). From factor Xa (FXa) programs, it is known that benzamidines suffer from low oral absorption as a result of the high pK_a and associated high desolvation energetics.[22] The basic benzamidine moiety is crucial for activity on the U-II receptor as shown by our pharmacophore model as well as in FXa for binding to the P1 pocket. Substitution of the benzamidine group by known biomimetics (e.g., aminoquinazoline and aminoindazole) has led to potent FXa inhibitors with good oral bioavailability.[23] A chemical optimization program focusing on benzamidine mimetics[24] is initiated to improve the pharmacokinetic profile of the discovered U-II receptor antagonists.

Conclusions

In the present study, the SAR derived for the physiological ligand and its NMR solution structure provided sufficient information to generate a pharmacophore model that proved to be useful for virtual screening; highly active chemical lead compounds of six different scaffold classes have been identified within the Aventis database showing antagonistic activity at the U-II receptor with a hit rate of 2.0% (number of active compounds/number of compounds tested × 100). This hit rate is about 20 times higher than seen in high throughput screens for GPCR antagonists. Recently, Marriott et al. successfully applied 3D database searching using a pharmacophore derived from known muscarinic M3 receptor antagonists for identifying novel candidate compounds.[25] However, the current work provides the first successful application of virtual screening based on a pharmacophore generated from SAR and NMR studies on the physiological peptidic ligand of its receptor. Virtual screening is thus a powerful method of quickly finding new nonpeptidic clinical leads even for peptide-binding GPCRs. The current example also reveals that the success of a virtual screening approach strongly depends on the quality of the pharmacophore model used for the 3D database search in chemical compound libraries.

Experimental Section

Materials. All peptides were purchased from Echaz Microcollections, Tübingen, Germany. CHO-K1 cells were obtained from the American Type culture collection (ATCC, Manassas, Virginia), cell culture media and sera were from GIBCO BRL (Gaithersburg, MD), the Ca fluorescent dye FLUO4 and pluronic acid were from Molecular devices (Sunnyvale, CA 94089-1136), oligonucleotides were from MWG-Biotech AG (Ebersberg, Germany), the gas chromatography (GC) melt polymerase chain reaction (PCR) kit was from Clontech (Palo Alto, CA), the expression plasmid pcDNA3.1 was from Invitrogen (Carlsbad, CA 92008), and competent *Escherischia coli* DH5α was from GIBCO.

Molecular Cloning of Human GPR14. As the putative human U-II sequence is intronless, we cloned the receptor from human genomic DNA (Clontech, Palo Alto, CA 94303-4230) via PCR. PCR conditions, established to amplify the GPR14 sequence, were 94 °C, 10 min followed by 35 cycles of 94 °C, 1 min, 60 °C, 1 min, 72 °C, and 2 min using the GC melt kit (Clontech). Primers designed to amplify the GPR14 sequence contained a *Bam*HI site in the forward and a *Xba*I site in the reverse primer, respectively. The urotensin receptor coding region, flanked by *Bam*HI/*Xba*I sites, was cloned into the pCDNA3.1(+) mammalian expression vector (Invitrogen, Carlsbad, CA) and sequenced in both directions.

Cell Culture and Transfection. CHO-K1 cells were cultured in basal ISCOVE medium (Biochrom) supplemented with 10% fetal bovine serum (Biochrom), penicillin−streptomycin (10 000 IU/mL−10 000 μg/mL; GIBCO), Gentamicin (Roche), and 2 mM L-glutamin (Roche). Cells were cultivated at 37 °C in a humidified 5% CO_2 incubator.

For transient transfections, 2×10^5 CHO-K1 cells were seeded into 35 mm dishes. About 24 h later, cells were transiently transfected at 50−80% confluency with 1 μg of GPR14 plasmid DNA per 35 mm dish using the LipofectAMINE Reagent (GIBCO) according to the manufacturer's instructions.

FLIPR Assay. Eighteen to twenty-four hours after transfection, CHO cells were seeded into 96 well plates at a density of 60 000 cells per well and cultured for 18−24 additional h until used in the functional FLIPR assays. Cells were then loaded with 95 μL of HBSS containing 20 mM Hepes, 2.5 mM probenecid, 4 μM fluorescent calcium indicator dye Fluo4 (Molecular Probes), and 1% fetal bovine serum for 1 h (37 °C, 5% CO_2). Cells were washed three times with phosphate-buffered saline containing 1 mM $MgCl_2$, 1mM ethylenediaminetetraacetic acid, and 2.5 mM probenecid in a Tecan cell washer. After the final wash, 100 μL of residual volume remained on the cells in each 96 well. Peptides were dissolved in DMSO as 2 mM stock solutions and diluted into the washing buffer described before prior to the assay as 3× solutions into 96 well plates. The FLIPR (Molecular Devices) was programmed to transfer 50 μL from each well of the ligand microplate to each well of the cell plate and to record fluorescence during 3 min in 1 s intervals during the first minute and 3 s intervals during the last 2 min. Peak fluorescence counts from the 18 to the 37 s time points are used to determine agonist activity. The instrument software normalizes the fluorescent reading to give equivalent initial readings at time zero.

NMR Spectroscopy. All NMR spectra were collected on a Bruker DRX 600 spectrometer operating at 600 MHz. All spectra were acquired at 27 °C using a solution of 5 mg of peptide in 0.6 mL of H_2O/D_2O (9:1). The data were processed on an indigo2 station (Silicon Graphics) with the XWINNMR

software from Bruker. Homonuclear experiments COSY,[26] TOCSY,[27] and ROESY[28] were performed with a spectral width of 12 ppm. In all of the experiments, spectra were recorded with 1024 increments in t_1 and 4096 complex data points in t_2. For the ROESY, 16 transients were averaged for each t_1 value, for COSY and TOCSY, eight transients. Mixing times of 70 or 150 ms were used for TOCSY (spin lock field 10 kHz, mixing sequence MLEV17) and ROESY spectra, respectively. Solvent suppression was achieved by a continuous irradiation during the recycle delay. Quantitative information on interproton distances were obtained from ROESY spectra (150 ms mixing time, spin lock field 3.00 kHz). The volume integrals of the individually assigned cross-peaks were converted into distance constraints using the isolated spin pair approximation (ISPA) and taking the offset effect into account.[29]

Structure Calculation. MD simulations and interactive modeling were performed using the software package SYBYL, version 6.6 (SYBYL Molecular Modeling Package, Version 6.6, Tripos, St. Louis, MO) on SGI workstations (Indigo 2, Power Challenge). All energy calculations were based on the Tripos 6.0 force field.[30] The rms distance (rmsd) between corresponding atoms in superimposed conformers was calculated using the MATCH command as implemented in Sybyl.

The experimental data sets used as input for the MD calculations included 57 distance constraints for U-II and 32 for the hexapeptide. For calibration, the following ROEs were set to a distance of 2.2 Å: for U-II, Asp^4-NH/Pro^3-Hα; for Ac-CFwKYC-NH_2, Lys^8-NH/$DTrp^7$-Hα. Upper and lower distance limits were set to plus and minus 10% of the calculated distances, respectively. For nondiastereotopically assigned methylene protons and methyl groups, 0.9 and 1.0 Å were added to the upper bounds as pseudoatom corrections, respectively.

The simulation protocol for U-II was as follows. After an initial energy minimization, the resulting structure was applied to a MD simulation for an equilibration period of 50 ps at 300 K with a time step of 1 fs. The ROE-derived distance constraints were applied with a force constant of 41.9 kJ/mol $Å^2$. The initial atomic velocities were assigned according to a Boltzmann distribution at 10 K. In the subsequent production run at 300 K, conformers were sampled every 50 ps for a duration of 300 ps yielding a total of six structures for further analysis. The obtained six structures were energy-minimized with a convergence criterion of 0.21 kJ/(mol Å). In the case of Ac-CFwKYC-NH_2, conformers were sampled every 50 ps for a duration of 500 ps yielding a total of 10 structures.

Generation of Pharmacophore. On the basis of the SAR studies presented within this paper, two three point pharmacophore hypotheses have been generated taking the NMR conformers of U-II and Ac-CFwKYC-NH_2 as a template (Catalyst version 4.5, Molecular Simulations, Inc.): A positive ionizable feature has been placed onto the Nϵ atom of Lys-8, and two hydrophobic aromatic features have been positioned onto the aryl rings of Trp-7 and Tyr-9, respectively (feature location constraint 1.5 Å). In addition, a shape query has been generated based on the truncated tripeptide Trp-Lys-Tyr as a template. The shape query was formed using the Catalyst default settings (similarity tolerance 0.5−1, percent box volume 0.7−1.3) and merged with the three point pharmacophore hypothesis derived for U-II and Ac-CFwKYC-NH_2, respectively.

Virtual Screening. A 3D Catalyst database has been generated comprising all compounds physically available within the compound library of Aventis. Each compound entry in the 3D database is covering a conformational model generated on an SGI power challenge by the "Conformation Generator Module" within Catalyst (fast generation type, energy range 20 kcal/mol of minimum). Using both three point pharmacophore hypotheses as 3D queries, the Aventis 3D Catalyst database was searched for small molecules, which match the pharmacophoric points of the physiological ligand (fast flexible mode).

Supporting Information Available: Chemical shifts and ROE data of U-II and Ac-CFwKYC-NH_2 are given. This material is available free of charge via the Internet at http://pubs.acs.org.

References

(1) Coulouarn, Y.; Lihrmann, I.; Jegou, S. Anouar, Y.; Tostivint, H.; Beauvillain, J. C.; Conlon, J. M.; Bern, H. A.; Vaudry, H. Cloning of the cDNA encoding the urotensin II precursor in frog and human reveals intense expression of the urotensin II gene in motoneurons of the spinal cord. *Proc. Natl. Acad. Sci. U.S.A.* **1998**, *95*, 15803−15808.

(2) Itoh, H.; McMaster, D.; Lederis, K. Functional receptors for fish neuropeptide urotensin II in major rat arteries. *Eur. J. Pharmacol.* **1988**, *149*, 61−66.

(3) Kumar, S.; Hedges, S. B. A molecular time scale for vertebrate evolution. *Nature* **1998**, *392*, 917−920.

(4) Ames, R. S.; Sarau, H. M.; Chambers, J. K.; Willette, R. N.; Aiyar, N. V.; Romanic, A. M.; Louden, C. S.; Foley, J. J.; Sauermelch, C. F.; Coatney, R. W.; Ao, Z.; Glover, G. J.; Wilson, S.; McNulty, D. E.; Ellis, C. E.; Elshourbagy, N. A.; Shabon, U.; Trill, J. J.; Hay, D. W. P.; Ohlstein, E. H.; Bergsma, D. J.; Douglas, S. A. Human Urotensin-II is a potent vasoconstrictor and agonist for the orphan receptor GPR14. *Nature* **1999**, *401*, 282−286.

(5) Liu, Q.; Pong, S.-S.; Zeng, Z.; Zhang, Q.; Howard, A. D.; Williams, D. L.; Davidoff, M.; Wang, R.; Austin, C. P.; McDonald, T. P.; Bai, C.; George, S. R.; Evans, J. F.; Caskey, C. T. Identification of urotensin II as the endogenous ligand for the orphan G-protein-coupled receptor GPR14. *Biochem. Biophys. Res. Commun.* **1999**, *266*, 174−178.

(6) Mori, M.; Sugo, T.; Abe, M.; Shimomura, Y.; Kurihara, M.; Kitada, C.; Kikuchi, K.; Shintani, Y.; Kurokawa, T.; Onda, H.; Nishimura, O.; Fujino, M. Urotensin II is the endogenous ligand of a G-protein coupled orphan receptor SENT (GPR 14). *Biochem. Biophys. Res. Commun.* **1999**, *265*, 123−129.

(7) Nothacker, H.-P.; Wang, Z.; McNeill, A. M.; Saito, Y.; Merten, S.; O'Dowd, B.; Duckles, S. P.; Civelli, O. Identification of the natural ligand of an orphan G-protein-coupled receptor involved in the regulation of vasoconstriction. *Nat. Cell Biol.* **1999**, *1*, 381−385.

(8) Gibson, A. Complex effects of Gillichthys urotensin II on rat aortic strips. *Br. J. Pharmacol.* **1987**, *91*, 205−212.

(9) Douglas, S. A.; Sulpizio, A. C.; Piercy, V.; Sarau, H. M.; Ames, R. S.; Aiyar, N. V.; Ohlstein, E. H.; Willette, R. N. Differential vasoconstrictor activity of human urotensin-II in vascular tissue isolated from the rat, mouse, dog, pig, marmorset and cynomolgus monkey. *Br. J. Pharmacol.* **2000**, *131*, 1262−1274.

(10) MacLean, M. R.; Alexander, D.; Stirrat, A.; Gallagher, M.; Douglas, S. A.; Ohlstein, E. H.; Morecroft, I.; Polland, K. Contractile responses to human urotensin-II in rat and human pulmonary arteries: effect of endothelial factors and chronic hypoxia in the rat. *Br. J. Pharmacol.* **2000**, *130*, 201−204.

(11) Maguire, J. J.; Kuc, R. E.; Davenport, A. P. Orphan-receptor ligand human urotensin II: receptor localization in human tissue and comparison of vasoconstrictor responses. *Br. J. Pharmacol.* **2000**, *131*, 441−446.

(12) Ithoh, H.; Itoh, Y.; River, J.; Lederis, K. Contraction of major artery segments of rat by fish neuropeptide urotensin II. *Am. Phys. Soc.* **1987**, *252*, R361−R366.

(13) Perkins, T. D. J.; Bansal, S.; Barlow, D. J. Molecular Modeling and design of analogues of the peptide hormone urotensin II. *Biochem. Soc. Trans.* **1990**, *18*, 8 (5), 918−919.

(14) Rohrer, S. P.; et al. Rapid Identification of Subtype-Selective Agoinsts of the Somatostatin Receptor Through Combinatorial Chemistry. *Science* **1998**, *282*, 737−740.

(15) Manning, M.; Stoev, S.; Cheng, L. L.; Wo, N. C.; Chan, W. Y. Synthesis and structure−activity investigation of novel vasopressin hypotensive peptide agonists. *J. Pept. Sci.* **1999**, *5*, 472−490.

(16) Lebl, M.; Hruby, V. J.; Castrucci, A.; Hadley, M. E. Melanin concentrating hormone analogues: Contraction of the cyclic structure. *Life Sci.* **1989**, *44*, 451−457.

(17) Audinot, V.; Beauverger, P.; Lahaye, C.; Suply, T.; Rodriguez, M.; Ouvry, C.; Lamamy, V.; Imbert, J.; Rique, H.; Nahon, J. L.; Galizzi, J. P.; Canet, E.; Levens, N.; Fauchère, J. L.; Boutin, J. A. Structure−activity relationship studies of melanin-concentrating hormone (MCH)-related peptide ligands at SLC-1, the human MCH receptor. *J. Biol. Chem.* **2001**, *276*, 13554−13562.

(18) Kinney, W. A.; Almond, H. R., Jr.; Maryanoff, B. E.; Qi, J.; Smith, C. E.; Santulli, R. J.; de Garavilla, L.; Andrade-Gordon, P.; Cho, D. S.; Everson, A. M.; Feinstein, M. A.; Leung, P. A. Structure−function study of the urotensin-II peptide: Elucidation of features required for potent agonist activity. *Abstracts of Papers*, 222nd American Chemical Society National Meeting, Chicago, IL, 2001; American Chemical Society: Washington, DC, 2001; MEDI-232.

(19) Wüthrich, K. *NMR of Proteins and Nucleic Acids*; Wiley: New York, 1986.
(20) Bhaskaran, R.; Arunkumar, A. I.; Yu, C. NMR and dynamical simulated annealing studies on the solution conformation of urotensin II. *Biochim. Biophys. Acta* **1994**, *1199*, 115−122.
(21) Lipinski, C. A.; Lombardo, F.; Dominy, B. W.; Feeney, P. J. Experimental and computational approaches to estimate solubility and permeability in drug discovery and development settings. *Adv. Drug Delivery Rev.* **1997**, *23*, 3−25.
(22) Lam, P. Y. S.; Li, R.; Clark, C. G.; Pinto, D. J.; Alexander, R. S.; Rossi, K. A.; Knapp, R. M.; Wong, P. C.; Aungst, B. J.; Bai, S. A.; Wright, M. R.; Wexler, R. R. Structure-based design and discovery of orally available potent nonbenzamidine factor Xa inhibitors. *Book of Abstracts*, 219th American Chemical Society National Meeting, San Francisco, CA, 2000; American Chemical Society: Washington, DC, 2000; MEDI-160.
(23) Li, R.; Clark, C. G.; Rossi, K. A.; Wang, P. C.; Luettgen, J. M.; Aungst, B. J.; Bai, S. A.; Knabb, R. M.; Wexler, R. R.; Lam, P. Y. S. Discovery of aminoquinazoline and aminoindazole P1 side chains as benzamidine mimics for Fxa inhibitors. *Abstr. Pap.—Am. Chem. Soc.* **2001**, *221*, MEDI-050.
(24) Masic, L. P.; Kikelj, D. Arginine mimetics. *Tetrahedron* **2001**, *57*, 7073−7105.
(25) Marriott, D. P.; Dougall, I. G.; Meghani, P.; Liu, Y.-J.; Flower, D. R. Lead Generation Using Pharmacophore Mapping and Three-Dimensional Database Searching: Application to Muscarinic M_3 Receptor Antagonists. *J. Med. Chem.* **1999**, *42*, 3210−3216.
(26) Marion, D.; Wüthrich, K. Application of phase sensitive two-dimensional correlated spectroscopy (COSY) for measurements of ^{1}H-^{1}H spin−spin coupling constants in proteins. *Biochem. Biophys. Res. Commun.* **1983**, *113*, 967−974.
(27) Bax, A.; Davis, D. G. MLEV-17-Based two-dimensional homonuclear magnetization transfer spectroscopy. *J. Magn. Reson.* **1985**, *65*, 355−360.
(28) Bothner-By, A. A.; Stephens, R. L.; Lee, J.; Warren, C. D.; Jeanloz, J. W. Structure determination of a tetrasaccharide: Transient Nuclear Overhauser Effects in the rotating frame. *J. Am. Chem. Soc.* **1984**, *106*, 811−813.
(29) Griesinger, C.; Ernst, R. R. Frequency offset effects and their elimination in NMR rotating frame cross-relaxation spectroscopy, *J. Magn. Reson.* **1987**, *75*, 261−271.
(30) Clark, M.; Cramer, R. D., III; Van Opdenbosch, N. Validation of the general purpose tripos 5.2 force field. *J. Comput. Chem.* **1989**, *10*, 982−1012.

JM0111043